Published OnlineFirst April 4, 2018; DOI: 10.1158/1078-0432.CCR-17-1898

Translational Cancer Mechanisms and Therapy

Clinical Cancer Research

Orthoxenografts of Testicular Germ Cell Tumors Demonstrate Genomic Changes Associated with Cisplatin Resistance and Identify PDMP as a Resensitizing Agent

Josep M. Piulats[1,2], August Vidal[3,4], Francisco J. García-Rodríguez[1,8], Clara Muñoz[1], Marga Nadal[1], Catia Moutinho[5], María Martínez-Iniesta[1], Josefina Mora[6], Agnés Figueras[1], Elisabet Guinó[7], Laura Padullés[1], Àlvaro Aytés[1], David G. Molleví[1], Sara Puertas[1], Carmen Martínez-Fernández[8], Wilmar Castillo[1], Merce Juliachs[1], Victor Moreno[7], Purificación Muñoz[5], Milica Stefanovic[9], Miguel A. Pujana[1], Enric Condom[3], Manel Esteller[5], Josep R. Germà[2], Gabriel Capella[1], Lourdes Farré[1,10,11], Albert Morales[7], Francesc Viñals[1,12], Xavier García-del-Muro[2], Julián Cerón[8,13], and Alberto Villanueva[1,13,4]

Abstract

Purpose: To investigate the genetic basis of cisplatin resistance as efficacy of cisplatin-based chemotherapy in the treatment of distinct malignancies is often hampered by intrinsic or acquired drug resistance of tumor cells.

Experimental Design: We produced 14 orthoxenograft transplanting human nonseminomatous testicular germ cell tumors (TGCT) in mice, keeping the primary tumor features in terms of genotype, phenotype, and sensitivity to cisplatin. Chromosomal and genetic alterations were evaluated in matched cisplatin-sensitive and their counterpart orthoxenografts that developed resistance to cisplatin in nude mice.

Results: Comparative genomic hybridization analyses of four matched orthoxenografts identified recurrent chromosomal rearrangements across cisplatin-resistant tumors in three of them, showing gains at 9q32-q33.1 region. We found a clinical correlation between the presence of 9q32-q33.1 gains in cisplatin-refractory patients and poorer overall survival (OS) in metastatic germ cell tumors. We studied the expression profile of the 60 genes located at that genomic region. *POLE3* and *AKNA* were the only two genes deregulated in resistant tumors harboring the 9q32-q33.1 gain. Moreover, other four genes (*GCS, ZNF883, CTR1,* and *FLJ31713*) were deregulated in all five resistant tumors independently of the 9q32-q33.1 amplification. RT-PCRs in tumors and functional analyses in *Caenorhabditis elegans* (*C. elegans*) indicate that the influence of 9q32-q33.1 genes in cisplatin resistance can be driven by either up- or down-regulation. We focused on glucosylceramide synthase (GCS) to demonstrate that the GCS inhibitor DL-threo-PDMP resensitizes cisplatin-resistant germline-derived orthoxenografts to cisplatin.

Conclusions: Orthoxenografts can be used preclinically not only to test the efficiency of drugs but also to identify prognosis markers and gene alterations acting as drivers of the acquired cisplatin resistance. *Clin Cancer Res; 24(15); 3755–66. ©2018 AACR.*

[1]Program Against Cancer Therapeutic Resistance (ProCURE), Catalan Institute of Oncology (ICO), Bellvitge Institute for Biomedical Research (IDIBELL), Oncobell Program, L'Hospitalet del Llobregat, Barcelona, Catalonia, Spain. [2]Department of Medical Oncology, Catalan Institute of Oncology (IDIBELL), Barcelona, Spain. [3]Department of Pathology, Hospital Universitari de Bellvitge (IDIBELL), CIBERONC, Barcelona, Spain. [4]Xenopat S.L., Business Bioincubator, Bellvitge Health Science Campus, L'Hospitalet de Llobregat, Barcelona, Spain. [5]Cancer Epigenetics and Cell Biology Program (PEBC), Catalan Institute of Oncology (IDIBELL), Barcelona, Spain. [6]Department of Biochemistry, Hospital de Sant Pau, Barcelona, Spain. [7]Bioinformatic Unit, Catalan Institute of Oncology (IDIBELL), Barcelona, Spain. [8]Modelling Human Diseases in *C. elegans*. Genes, Disease and Therapy Program (IDIBELL), Barcelona, Spain. [9]Department of Cell Death and Proliferation, Instituto de Investigaciones Biomédicas de Barcelona (IIBB-CSIC), IDIBAPS, L'Hospitalet de Llobregat, Barcelona, Catalonia, Spain. [10]Laboratory of Experimental Pathology (LAPEX), Gonçalo Moniz Research Center, Oswaldo Cruz Foundation (CPQGM/FIOCRUZ), Salvador, Bahia, Brazil. [11]Institute of Science and Technology of Tropical Diseases (INCT/DT), Salvador, Brazil. [12]Departament de Ciencies Fisiologiques II, Universitat de Barcelona, L'Hospitalet de Llobregat, Barcelona, Spain. [13]C. elegans Core Facilty-IDIBELL, Barcelona, Spain.

Note: Supplementary data for this article are available at Clinical Cancer Research Online (http://clincancerres.aacrjournals.org/).

J.M. Piulats and A. Vidal contributed equally to this article.

Corresponding Authors: Alberto Villanueva, Catalan Institute of Oncology (ICO/IDIBELL), Hospital Duran i Reynals, 3a planta - Gran Via de l'Hospitalet, 199, L'Hospitalet de Llobregat, Barcelona 08908, Spain. Phone: 349-3260-7952; Fax: 349-3260-7466; E-mail: avillanueva@iconcologia.net; and Julián Cerón, Bellvitge Institute for Biomedical Research (IDIBELL),Hospital Duran i Reynals, 3a planta - Gran Via de l'Hospitalet, 199, L'Hospitalet de Llobregat, Barcelona 08907, Spain. Phone: 349-3260-7287; jceron@idibell.cat.

doi: 10.1158/1078-0432.CCR-17-1898

©2018 American Association for Cancer Research.

Downloaded from clincancerres.aacrjournals.org on April 16, 2021. © 2018 American Association for Cancer Research.

Published OnlineFirst April 4, 2018; DOI: 10.1158/1078-0432.CCR-17-1898

Translational Relevance

Cisplatin-based cytotoxic chemotherapy is the mainstay of the treatment of several types of neoplasias. The acquired resistance is a major clinical limitation for patient's survival. Orthoxenografts are the most advanced *ex vivo* platforms to investigate the efficiency of drugs in a personalized manner, but in this study, we also demonstrated other valuable tools to identify prognosis markers and novel resensitizing therapeutic approaches for the treatment of cisplatin-refractory tumors. As proof-of-principle, in this study we validate our approach demonstrating that presence of the 9q32-q33.1 gain is associated with poor risk defined by shorter overall survival (OS) and that genetic or pharmacologic inhibition of glucosylceramide synthase (GCS) activity is efficient to resensitize testicular and epithelial ovarian tumors refractory to cisplatin.

Introduction

Testicular germ cell tumors (TGCT) of adolescent and young adults are the most common malignancy in young men (1–3). They can be classified as seminomas (SE; originated in epithelium of the seminiferous tubules), which represent around 40% of cases, and nonseminomas (NSE; 60%). Seminomas are radio- and chemo-sensitive tumors highly curable at all stages. With the exception of teratomas, NSEs are also highly sensitive to cisplatin-based chemotherapy and, when combined with surgery, patients achieve high cure rates (4). In contrast with most advanced solid tumors, approximately 80%–90% of metastatic TGCTs will achieve complete cure after standard doses of cisplatin (CDDP) chemotherapy (4). Nevertheless, 10%–15% of patients die due to cisplatin refractoriness and the absence of alternative effective resensitizing therapies (5–7). Such high success in treating advanced testicular cancer has limited the number of studies addressing the treatment failure in refractory patients (8, 9).

In TGCTs, cisplatin resistance has been attributed to diverse cellular mechanisms (10–12), although the molecular details underlying treatment failure in refractory patients remains obscure (13–17). Patient-derived orthotopic xenografts, named PDOX or orthoxenografts, are relevant preclinical animal models that phenocopy human tumor properties (18,19). We have previously used TGCT orthoxenografts to explore novel therapeutic approaches for refractory TGCTs (20, 21). In this study, the genetic basis of acquired cisplatin resistance was investigated by comparative genomic hybridization (CGH) in a collection of matched cisplatin-sensitive and -resistant NSE tumors that were implanted orthotopically in nude mice. We studied genome amplifications and further investigated the 9q32-q33.1 region to identify cisplatin resistance–related genes. We found a clinical correlation between the presence of the 9q32-q33.1 gain and poor risk defined by shorter overall survival (OS). We also found gene expression alterations within the 9q32-q33.1 region that were associated with cisplatin resistance but not necessarily with the 9q32-q33.1 gain. Finally, we used a drug to inhibit one of the recurrently upregulated genes in cisplatin-refractory tumors, the glucosylceramide synthase (GCS), and observed that tumors were resensitized allowing the maintenance of the cisplatin-based therapy.

Materials and Methods

Human primary TGCT implantation and perpetuation in nude mice

To generate the collection of TGCT orthoxenografts, fresh surgical specimens of 62 human GCTs were implanted in nude mice. Twenty-two tumors were classified as pure SEs and 40 as NSE (21 as pure and 19 as mixed tumors containing different proportions of SE and NSE components). From the 40 NSEs, 14 tumors were perpetuated (35%), 10 derived from pure NSEs [three choriocarcinomas (CH), four embryonal carcinomas (EC), three yolk sac tumors (YS)], and four from mixed primary tumors. Five orthoxenografts were derived from several extragonadal tumor locations, and in four cases from patients treated previously with cisplatin-based chemotherapy (Supplementary Table S1). None of the 22 implanted pure gonadal seminomas (SE) grew in nude mice. Of the mixed tumors, comprising both SE and NSE components, only the NSEs grew in mice. Orthotopic implantation procedure of human tumors was performed as previously reported by our group (21) and briefly described in the Supplementary Data. IHC characterization is also described in the Supplementary Data. All patients gave written consent to participate in the study. The Institutional Ethics Committees approved the study protocol, and the animal experimental design was approved by the IDIBELL animal facility committee (AAALAC – Unit 1155). All experiments were performed in accordance with the guidelines for Ethical Conduct in the Care and Use of Animals as stated in The International Guiding Principles for Biomedical Research Involving Animals, developed by the Council for International Organizations of Medical Sciences.

Generation in mice of refractory engrafted NSEs to cisplatin treatment

Five selected engrafted tumors, TGT1X, TGT12X, TGT21XB, TGT34X and TGT38X, from patients without prior exposure to cisplatin, were allowed to grow until intraabdominal palpable masses were noted. Animals were administered with cisplatin intravenously at a dose of 2 mg/kg for 3 consecutive weeks (days 0, 7, and 14; cycle #1 of treatment). Post-cisplatin relapse, tumors were harvested, prepared as described previously and engrafted in new animals. This process was repeated up to five times by treating tumor-bearing mice with stepwise increasing doses of cisplatin: cycle #2, 3 mg/kg; cycle #3, 3.5 mg/kg; cycle #4, 4 mg/kg; and cycle #5, 5 mg/kg, as we described for ovarian tumors (22). When mice were treated at doses higher than 3.5 mg/kg, the signs of cisplatin-induced toxicity were ameliorated by administration of saline containing 5% glucose for 2 days. Dynamic CDDP responses were evaluated after assessing β-hCG and/or AFP serum levels, as described in Supplementary Data.

Analysis of point mutations and genomic imbalances

The presence of point mutations in a panel of selected cancer-related genes and microsatellite instability (MSI) were compared between sensitive and resistant paired orthoxenografts. Procedures are described in detail in the Supplementary Data.

Whole-genome analysis by NimbleGen CGH arrays

The CGH oligonucleotide array was carried out by NimbleGen Systems, Inc., at their facility in Wisconsin. Array design descriptions were: 2006-07-27_HG18_WG_CGH, single array CGH design for whole-human genome (hg18; NCBI Build 36).

Downloaded from clincancerres.aacrjournals.org on April 16, 2021. © 2018 American Association for Cancer Research.

Published OnlineFirst April 4, 2018; DOI: 10.1158/1078-0432.CCR-17-1898

Methods of DNA labeling array construction, hybridization, array normalization, and data analysis have been described in detail by Seltzer and colleagues (23).

Patients

Eighty-eight consecutive patients diagnosed with metastatic germ cell tumors and treated at the Institut Català d'Oncologia (Barcelona, Spain) between 1989 and 2004 were initially included in this study. Thirteen cases were not evaluated because of the lack of paraffin-embedded tissue blocks. Patient demographics and clinical characteristics of the 75 patients finally evaluated are listed in Supplementary Table S3. Sixty-three patients (84%) had NSE tumors and 12 (16%) had SE tumors. Four patients presented with mediastinal extragonadal disease. Sixty percent of the patients were classified as having a good prognosis, 19% as having an intermediate prognosis, and 21% as being of poor prognosis according to the IGCCCG categorization. Twenty-four patients were considered resistant, defined by progression or relapse despite adequate first-line chemotherapy treatment. Cases with mature teratoma only in the resected postchemotherapy mass and without posterior tumor relapse were considered sensitive. Tumor samples from primary tumors and/or resected metastases obtained before chemotherapy were included in a newly generated tissue microarray (TMA), as described previously (24). FISH analysis was described in Supplementary Material.

Quantitative gene and miRNA analysis

Total RNA was extracted using TRIzol (Invitrogen), following the manufacturer's instructions, and reverse-transcribed to cDNA. Quantitative RNA and miRNA analyses were performed as described in the Supplementary Material.

Cell culture, transfection and *in vitro* gene overexpression, and shRNAi knockdown experiments

The human NSE cell lines SuSaS (of teratocarcinoma origin) and its matched SuSaR ("R" for CDDP-resistant derived cell line) were grown for different experiments as described previously (25). For overexpression experiments, SuSaS cells were transfected with plasmid pCMV6-XL5-GCS containing the whole GCS human cDNA from OriGene (SC118052). Knockdown experiments were realized in SuSaR with four predesigned short hairpin RNAs (shRNA) for the human GCS gene from Qiagen (KH02376P) that were transfected with the jetPrime transfection kit (Polyplus), following manufacturer's instructions. GCS expression levels were analyzed by Western blot analysis at 24, 48, 72, and 96 hours posttransfection by anti-GCS (1/1,000; Protein-Tech) using anti-β-actin-HRP antibody as a control (1/20,000; Sigma-Aldrich). The chosen time to perform the experiments was 48 hours.

In vitro determination of drug resistance assays

Cisplatin (1 mg/mL) dissolved in NaCl (TEVA) and DL-threo-PDMP (Sigma-Aldrich) in DMSO at a final concentration of 59 mmol/L were assessed. Cell viability was determined by MTT assay. Briefly, 1×10^3 cells were plated onto 96-well plates, after 4 hours of transfection, fresh medium was added and cells were treated for 48 hours with different drugs concentration ranged from 0 to 20 μg/mL doses. MTT was added at a final concentration of 0.1% and after 2.5 hours of incubation (37°C, 5% CO_2) metabolic product formazan was dissolved in DMSO and the absorbance measured at 570 nm. Prism Software was used to calculate half maximal inhibitory concentration (IC_{50}) of the drugs.

Determination of GCS activity

Tumor samples were homogenized in lysis buffer (Tris-HCl 10 mmol/L, EDTA 1 mmol/L, and 0.1% Triton X-100 at pH 7.4) and centrifuged at 600 × *g* for 5 minutes. GCS activity was determined from NBD-C6-ceramide and UDP-glucose, the conversion product separated by TLC with chloroform/methanol/32% ammonia (70:30:5, v/v), and quantified by densitometry (Préférence/DVS, Sebia) as described previously (26). Briefly, for each assay, 200 μg of protein extract was suspended in reaction buffer (5 mmol/L $MgCl_2$, 5 mmol/L $MnCl_2$, and 1 mmol/L EDTA in 50 mmol/L HEPES, pH 7.2) and the substrate mixture containing 10 μmol/L NBD-C6-ceramide and 250 μmol/L UDP-glucose. After a 30-minute incubation at 37°C, reactions were terminated by adding 2.5 mL of chloroform/methanol (2:1, v/v), the samples were centrifuged (1,000 × *g*, 5 minutes), the lower phases dried under nitrogen, and subjected to TLC by using chloroform/methanol/32% ammonia (70:30:5, v/v) as the mobile phase.

Evaluation of *in vivo* responses of cisplatin-refractory orthoxenografts to treatment with DL-threo-PMDP

Tumors were implanted in mouse testicle and when homogeneous tumor sizes were detected, animals were randomized to four treatment groups ($n = 6$–8 mice/group): (i) vehicle; (ii) cisplatin (3.5 mg/kg); (iii) DL-threo-PDMP(D-threo-1-phenyl-2-decanoylamino-3-morpholino-1-propanol hydrochloride; Santa Cruz Biotechnology), 50 mg/kg dissolved in 5% of Tween 80%–0.85% NaCl; and (iv) DL-threo-PDMP+cisplatin (50 mg/kg+ 3.5 mg/kg). Cisplatin was intravenously administered once a week for three consecutive weeks (days 0, 7, and 14), while DL-threo-PDMP was administered daily by intraperitoneal injection over the 21-day period and mice were sacrificed on day 22 of treatment. In combined treatments, PDMP was administered one hour before cisplatin treatment. Ovarian orthoxenograft 17 model (OVA17X) was generated from a cisplatin-sensitive human serous epithelial ovarian tumor by orthotopic implantation (in the mouse ovary) in nude mice, as described previously (22). Cisplatin-resistant ovarian orthoxenograft 17 (OVA17XR) was derived from OVA17X by iterative treatment cycles with increasing doses of cisplatin, as described above for TGCT tumors. For the *in vivo* treatment with DL-threo-PMDP, OVA17XR was grown and implanted in the mouse ovary of several animals. When homogeneous tumor sizes were detected, they were randomized to four treatment groups ($n = 6$ mice/group) and treated as described previously.

Statistical analysis

For the clinicopathologic features, *P* values were calculated using the χ^2 test. Survival curves were estimated using the Kaplan–Meier method, and differences between individual curves were evaluated by multivariate Cox proportional hazards regression modeling. Analyses were adjusted for pathologic diagnostic classification. HRs and 95% confidence intervals (CI) were calculated. Likelihood ratio tests were used to assess the prognostic value of genomic amplification of 9q32-q33.1 by FISH in the TMA of metastatic GCTs. Values of $P < 0.05$ were considered significant.

Downloaded from clincancerres.aacrjournals.org on April 16, 2021. © 2018 American Association for Cancer Research.

Published OnlineFirst April 4, 2018; DOI: 10.1158/1078-0432.CCR-17-1898

Results

Establisment of orthoxenografts of TGCT NSE tumors

To study cisplatin resistance in TGCTs, our laboratory has compiled a valuable collection ($n = 14$) of both cisplatin-sensitive and -refractory TGCT NSE orthoxenografts (Supplementary Table S1). These orthoxenografts grew on mouse testicles as a big solid mass, displaying a strong correlation with their corresponding primary tumors in terms of histological appearance and expression of cellular markers (Fig. 1A and B). These tumors were kept stable throughout serial passages and, as occurring in patients, the secreted beta subunit of human chorionic gonadotropin (β-hCG) and/or alpha-fetoprotein (AFP) were detected in mouse serum as surrogate markers of tumor growth (Supplementary Table S1; refs. 27, 28).

Orthoxenografts reproduce in mice some of the patterns of dissemination observed in humans with the presence of retroperitoneal lymph nodes, lungs, and liver metastasis. Rare brain metastases were not detected in mice. Distant from what happens in humans in two tumors, we have detected the presence of peritoneal implants (Supplementary Table S1).

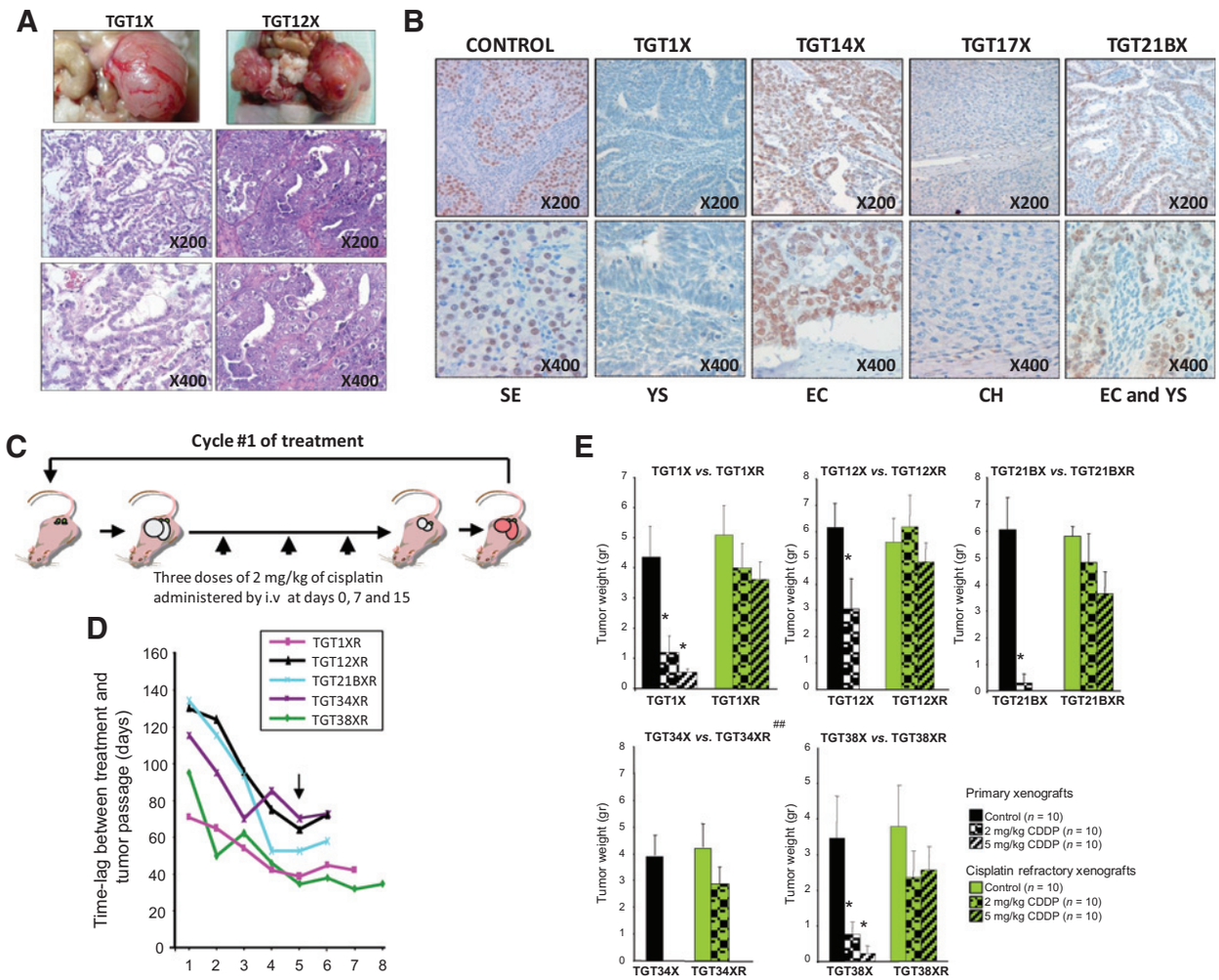

Figure 1.

Generation of TGCT orthoxenografts and development of paired cisplatin-refractory tumors. **A,** Macroscopic appearance and hematoxylin and eosin (H&E) staining of mice with orthoxenografts (left, TGT1X pure yolk sac, right, TGT12X pure embryonal carcinoma). **B,** OCT4 protein immunostaining. High levels of nuclear staining were only identified in TGT14X, pure embryonal carcinoma (EC) and TGT21BX, mixed EC and yolk sac tumor (YS). Absence of protein expression was noted in TGT1X, pure YS and TGT17X, pure choriocarcinoma (CH). Seminoma (SE) was used as a positive control. **C,** Generation of engrafted tumors refractory to cisplatin treatment combines: (i) five cycles of repetitive cisplatin treatments (one cycle: 3 doses of cisplatin administered by intravenous injection for three consecutive weeks, on days 0, 7, and 14) each cycle performed in diferent animals and (ii) doses of cisplatin were increased after each cycle of treatment ranging from 2 mg/kg (first cycle) to 5 (fifth cycle). **D,** The time lag between tumor-treatment and tumor-regrowth decreased as the different treatment cycles occurred. Tumors at cycle #5 of treatment (arrow) were used to assess the response to chemotherapy. **E,** Comparative short-term cisplatin response assays for paired nontreated versus cisplatin-resistant tumor. Mice were treated with low (2 mg/kg) and high (5 mg/kg) doses of cisplatin. TGT21BX and TGT34X showed a complete response at high doses. ##, for paired TGT34X versus TGT34XR, only the response to the low dose was assessed (*, $P < 0.05$).

Downloaded from clincancerres.aacrjournals.org on April 16, 2021. © 2018 American Association for Cancer Research.

Published OnlineFirst April 4, 2018; DOI: 10.1158/1078-0432.CCR-17-1898

Orthoxenografts of NSE recapitulate the responses to cisplatin treatment in humans

We studied the pattern of responses to chemotherapy for nine orthoxenografts. Mice were treated with low (2 mg/kg) and high (5 mg/kg) doses of cisplatin, and their short- and long-term responses were evaluated. All tumors had a good short-term response to low doses of cisplatin, as indicated by a significant reduction in tumor weight in 8 cases and complete response in the tumor TGT21BX (Supplementary Fig. S1). A good correlation between tumor weight and reduction or absence of serum β-hCG and/or AFP levels was found, supporting its use as a dynamic surrogate marker of treatment efficacy. Differences among tumor weight and serum markers observed in TGT21AX after treatment can be explained by the predominance of a teratoma with a few microscopic islands of viable cells (Supplementary Fig. S1C). Administration of higher doses of cisplatin (5 mg/kg) was associated with a better response in all cases (Supplementary Fig. S1). In addition, there was a complete response in tumor TGT21AX (Supplementary Fig. S1C).

To investigate long-term cisplatin responses, a subgroup of the treated mice was kept alive postchemotherapy until tumor regrowth was observed. Tumors regrew in 8 of 9 cases, over a period of 15 to 135 days, independently of the cisplatin dose in most instances (Supplementary Fig. S1). In TGT39X, both treatments yielded a long and sustained response, as was confirmed by constant levels of AFP over a latency period of 90 days (Supplementary Fig. S1A). Histologic analysis of relapsed masses demonstrated the presence of a viable tumor in most cases, and the maintenance of the tumor heterogeneity, observed in mixed nontreated tumors (Supplementary Fig. S2). As observed in patients, cisplatin induced increasing teratoma differentiation in TGT21AX (Supplementary Figs. S1C, bottom S2).

Development of matched models of cisplatin refractoriness

To investigate cisplatin resistance against the same genetic background (sensitive vs. resistant), we developed several cisplatin-refractory tumor models. Thus, from this collection of 14 tumors, to develop this study, we selected 5 that were not exposed to cisplatin before implantation. This subset includes a YS (TGT1X), two embryonal carcinomas (TGT12X and TGT34X), a choriocarcinoma (TGT38X), and a mixed tumor (TGT21BX; Supplementary Table S1). Through five iterative cycles of treatment in different mice, and applying increasing doses of cisplatin through the cycles, we generated orthoxenografts with acquired resistance *in vivo* (named TGT1XR, TGT12XR, TGT21BXR, TGT34XR, and TGT38XR; Fig. 1C). During the process of resistance acquisition, a progressive shortened time lag between tumor treatment and tumor regrowth was noted, and the mice to mice passage time stabilized after five cycles of treatment in all cases (Fig. 1D). To evaluate the resistance to cisplatin in these transplanted tumors, paired short-term response assays between untreated (TGTX) and resistant (TGTXR) tumors at cycle #5 were performed (Fig. 1E). High levels of resistance were observed in all tumors at both low (2 mg/kg) and high (5 mg/kg) cisplatin doses. Finally, supporting the experimental value of this collection of paired sensitive/resistant orthoxenografts, we observed similar histologic pattern between original and cisplatin-resistant tumors (Supplementary Fig. S2).

Recurrent chromosomal imbalances were associated with acquired cisplatin resistance

In the DNA, cisplatin induces interstrand crosslinks and monoadducts that cause mutations and genomic instability (11, 29). Many of these alterations on the cisplatin-exposed DNA cannot be repaired and cause cellular lethality, but some may be selected and promote the cellular resistance to cisplatin. Thus, we investigated in paired TGCT orthoxenografts (sensitive vs. resistant) with the same genetic background whether the acquisition of cisplatin resistance was associated with the selection of specific genomic imbalances or mutations in a panel of selected genes. First, we did not find mutations in a subset of cancer-related genes including *K-ras*, *b-raf*, *PI3KCA*, *EGFR*, *c-Kit*, *PDGFRα* and *β*, *p15*, *p16*, and *SMAD4* or changes in the MSI status in resistant engrafted tumors. Then, we investigated chromosomal rearrangements, using array-based CGH, in four paired untreated parental engrafted tumors and their resistant counterparts (TGT1XR was later tested for 9q32-q33.1 amplification only). Few recurrent genomic changes were consistently detected in distinct resistant tumors when compared with their paired sensitive orthoxenograft (Fig. 2A). Particularly, gains at 9q were found in three of four cases, 9q32-q33.1 being the smallest common gain (5.1 M bp containing 60 genes) between three resistant tumors (Fig. 2B). In addition, gains at 15q23-q24.1 and 15q26.3 were identified in two tumors, and the loss of the Xp22.33 region was identified in three of four tumors (Supplementary Fig. S3). All these four genomic regions are hotspots to search for genes involved in the acquired resistance to cisplatin. In this study, we focused our attention on studying the 9q32-q33.1 region.

Amplification at 9q32-q33.1 is associated with an increased risk of death in advanced TGCT patients

To evaluate the clinical relevance of our results in orthoxenografts, gains at 9q32-q33.1 were studied by FISH in a human TMA including series of tumors from 75 patients with metastatic TGCTs (63 NSEs and 12 SEs) homogeneously treated with cisplatin-based chemotherapy in our hospital (Fig. 2C; Supplementary Table S2). Amplification at 9q32-q33.1 was identified in 18 of 75 (24%) cases, including 16 NSEs (5 CEs, 2 CHs, 1 YS, 2 TEs, and 6 mixed tumors) and two pure SEs (Table 1). Analysis of OS showed that amplification at the 9q32-q33.1 region was associated with a 2.79-fold greater risk of death in patients with metastatic GCTs ($P = 0.036$; HR = 2.79; 95% CI = 1.11–7.0; Table 1 and Fig. 2D). A higher risk of death associated to this genetic amplification was revealed when considering only patients with NSE ($n = 63$; $P = 0.026$; HR = 3.03; 95% CI = 1.18–7.76), but there was no difference in those with SE ($P = 0.54$; Table 1). OS subgroup analyses in NSE patients (presence of amplification vs. WT) showed a trend for good and intermediate risk groups alone; the relationship was statistically significant when we analyzed the two groups together ($P = 0.014$; HR = 5.16; 95% CI = 1.47–18.12; Table 1). This genetic amplification was also associated with shorter progression-free survival (PFS; $P = 0.043$; HR = 2.46; 95% CI = 1.07–5.63; Table 1; Fig. 2D) and such correlation was significant even when the NSE group alone was analyzed ($P = 0.024$, HR = 2.8, 95% CI = 1.19–6.57).

Moreover, there was a trend for tumors harboring the 9q32-q33.1 amplification to have a worse cisplatin response (Supplementary Table S3). Fifty percent of tumors with the

Downloaded from clincancerres.aacrjournals.org on April 16, 2021. © 2018 American Association for Cancer Research.

Published OnlineFirst April 4, 2018; DOI: 10.1158/1078-0432.CCR-17-1898

A

Tumor	Histology of resistant tumor [b]	Chromosome region [c]	Status	Scores [a]	Region	Size (Mbp)	Number of genes [d]
TGT12R	EC	9q21.11-q33.3	gain	+ 0.31	67.950 K - 123.690 K	55.7	502
		15q23-q24.1	gain	+ 0.36	69.690 K - 71.430 K	1.74	26
		15q26.3	gain	+ 0.37	97.770 K - 98.310 K	0.54	6
		Xp22.33	loss	- 0.29	30 K - 2.730 K	2.70	25
TGT21BR	YS, EC and CH	5p15.33-p15.2	gain	+ 0.30	90 K - 15.090 K	15.0	94
		9q21.11-q33.3	gain	+ 0.39	70.170 K - 123.690 K	53.5	461
		15q23-q24.1	gain	+ 0.39	69.690 K - 71.370 K	1.68	25
		15q24.3	gain	+ 0.30	74.970 K - 75.750 K	0.78	9
		15q26.3	gain	+ 0.41	97.830 K - 98.310 K	0.48	6
		Chromosome 21	gain	+ 0.28	0 K - 47.000 K	47	386
		Xp22.33	loss	- 0.45	30 K - 2.730 K	2.70	25
		Xp22.2	loss	- 0.42	9.510 K - 9.870 K	0.36	4
TGT34R	EC	No changes					
TGT38R	CH	9q32-q33.1	gain	+ 0.35	112.950 K - 118.050 K	5.10	60
		16p11.2-p11.1	gain	+ 0.34	34.350 K - 34.590 K	0.24	11
		20q13.13-q13.2	gain	+ 0.25	49.050 K- 49.770 K	0.72	5
		Xp22.23	loss	- 0.41	30 K - 2.730 K	2.70	25

[a] NimbleGen microarray data processed at 60 kbp average window. All the chromosomal gains or losses had a $\log_2$ score ≥0.30 or ≤0.30. No microarray data were available for TGT1R, a pure YS.
[b] Tumor histology: YS, yolk sac tumor, EC, embryonal carcinoma, CH, choriocarcinoma.
[c] Genomic changes were consistently detected in chemoresistant tumors at cycles #3 and #5 of chemotherapy.
[d] Location of genes in each region was based on build 36.3 from NCI.

B

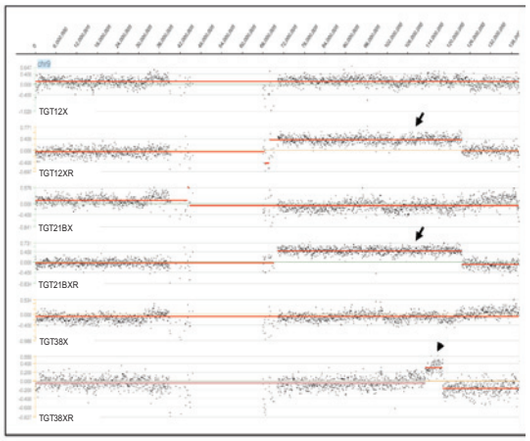

C

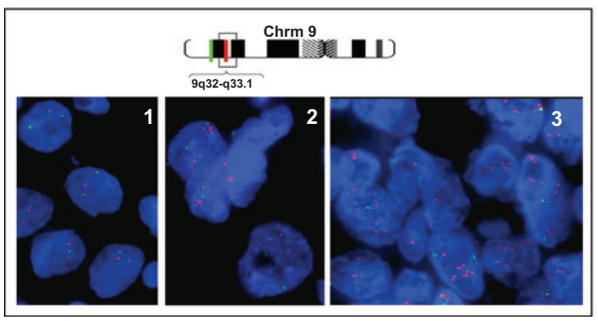

D

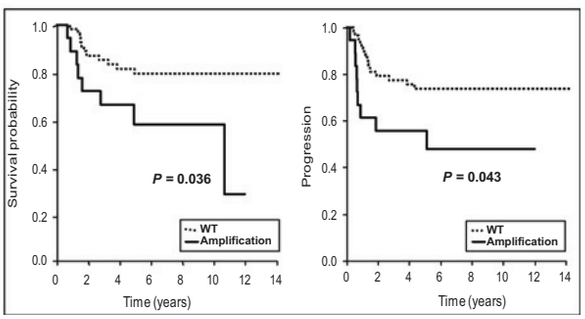

Figure 2.

Recurrent gains at 9q in refractory tumors. **A,** Chromosomal rearrangements related to acquired cisplatin resistance were identified when compared with four paired untreated parental engrafted tumors and their resistant counterparts. Whole-genome mapping was performed by oligonucleotide array CGH analysis (60 kbp window averaging) and visually depicted with the SignalMap graphical interface tool from Nimblegen Systems. **B,** The 9q21.11-q33.3 gain region (arrow) was identified in TGT12XR and TGT21BXR, while in tumor TGT38XR, there was a smaller overlapping region of 5.1 Mbp at 9q32-q33.1 (arrowhead). **C,** Representative FISH analyses of the copy number of 9q32-q33.1 in human metastatic CGT samples contained in the TMA. Interphase FISH with RP11-582I20 (red) and RP11-616C16 (green) probes. Panel 1: absence of amplification characterized by two red and two green signals in all interphase nuclei. Panels 2 and 3: amplification of the region. **D,** Kaplan–Meier plots by status of 9q32-q33.1 gains. Left, OS; right, PFS. *P* values are those from multivariate Cox proportional hazards regression models, controlling for the pathologic diagnostic classification.

amplification (9/18) were considered resistant to first-line chemotherapy compared with 26.3% (15/57) of tumors without it ($P = 0.060$). Up to 27.8% of tumors with the 9q32-q33.1 amplification did not achieve a tumor marker complete response or progressed during first-line treatment ($P = 0.007$; Supplementary Table S4).

Identification of 9q32-q33.1 genes whose expression is associated with tumor response to cisplatin

Next, to identify which genes within 9q32-q33.1 region could be related to cisplatin resistance, we performed quantitative PCR (qPCR) to study the expression levels of 60 genes and two miRNAs in the five paired sensitive/resistant engrafted tumors (Fig. 3A). In order to better represent our study of resistant tumors without the 9q32-q33.1 amplification, we included the pair TGT1X/TGT1XR in the gene expression profiling of this region to get a panel of three with and two without the 9q32-q33.1 gain. By qPCR, we found that 37 9q32-q33.1 genes, and the two miRNAs, were expressed in these five TGCTs (Fig. 3A and B). From these gene expression analyses, we observed that only two genes, *POLE3* and *AKNA*, were differently regulated in relation to the presence or absence of 9q32-q33.1 amplification. Interestingly, *POLE3* was upregulated in resistant tumors with 9q32-q33.1 gains, but downregulated in the two others without this genetic alteration. *AKNA* was downregulated in resistant tumors with 9q32-q33.1 gains, but not altered in the other two tumors without this alteration. Moreover, these results also indicate that a chromosomal gain does not necessarily mean gain of functions. Moreover, another five genes [*UGCG* (also known as *GCS*), *ZNF883*, *CTR1*, *ATP6V1G1*, and *FLJ31713*] were consistently up- or downregulated in all five resistant tumors independently of the 9q32-q33.1 amplification.

Downloaded from clincancerres.aacrjournals.org on April 16, 2021. © 2018 American Association for Cancer Research.

Published OnlineFirst April 4, 2018; DOI: 10.1158/1078-0432.CCR-17-1898

Table 1. Analysis of 9q32-q33.1 amplification in metastatic germ cell tumors

		Overall survival		Progression-free survival	
	N (%)	HR (95% CI)	*P*	HR (95% CI)	*P*
Chromosome copy number at 9q31-q32.1 ($n = 75$)					
WT	57 (76)	1	0.036[a]	1	0.043[a]
Amplification	18 (24)	2.79 (1.11–7.0)		2.46 (1.07–5.63)	
Stratified analysis					
Pathologic classification					
Nonseminoma ($n = 63$)					
WT	47 (74.6)	1	0.026[a]	1	0.024[a]
Amplification	16 (25.4)	3.03 (1.18–7.76)		2.8 (1.19–6.57)	
Seminoma ($n = 12$)					
WT	10 (83.3)	1 (0–Inf)	0.54	1 (0–Inf)	0.38
Amplification	2 (16.7)	0		0	
IGCCCG classification					
NSE with good risk ($n = 33$)					
WT	27 (81.8)	1	0.096	1	0.22
Amplification	6 (18.2)	5.89 (0.82–42.52)		3.29 (0.55–19.71)	
NSE with intermediate risk ($n = 14$)					
WT	10 (71.4)	1	0.15	1	0.28
Amplification	4 (28.6)	3.41 (0.68–17.02)		2.33 (0.52–10.44)	
NSE with poor risk ($n = 16$)					
WT	10 (62.5)	1	0.88	1	0.30
Amplification	6 (37.5)	0.9 (0.21–3.79)		2 (0.55–7.21)	
Grouping NSE according to good and intermediate risk ($n = 47$)					
WT	37 (78.7)	1	0.014 [a]	1	
Amplification	10 (21.3)	5.16 (1.47–18.12)		3.28 (1.03–10.37)	0.056

Abbreviation: WT, no amplification at 9q32-33.1.
[a]*P* values are from multivariate Cox models adjusted for pathological diagnostic classification.

Therefore, we found that gene expression changes at the 9q32-q33.1 region in resistant tumors were not necessarily correlated with the presence of the amplification, suggesting the coexistence of other mechanisms modifying gene expression that confer resistance to cisplatin.

The influence of genetic changes on resistant tumors is complex and multifactorial as reflected by the fact that the functional network (obtained from the web-based tool STRING) for 34 genes differentially expressed in these resistant tumors was rather poor (30), indicating a low functional relation between these genes. Importantly, the six genes showing deregulation in resistant tumors do not show any functional link (Supplementary Fig. S4).

Some gene functions involved in cisplatin response are conserved in *C. elegans*

We wondered whether the 9q32-q33.1 genes deregulated in resistant tumors were acting in the same manner in the response to cisplatin. Cisplatin has a broad mode of action being also toxic to eukaryotic cells of model organisms as *Caenorhabditis elegans* (*C. elegans*; ref. 31). We found that three of the five genes deregulated in resistant tumors (*GCS*, *CTR1*, and *ATP6V1G1*) were conserved in *C. elegans*. Through an automated toxicity assay, we found that *vha*-10/ATP6V1G1(RNAi) animals were sensitive to cisplatin (Supplementary Fig. S5). *GCS* present three paralogs in *C. elegans* and we needed to inactivate two of them at the time to produce sensitivity to cisplatin. On the contrary, worms treated with CTR1/F27C1.2(RNAi) were resistant to cisplatin exposure, as expected from the inactivation of the cooper transporter that is involved in cellular intake of cisplatin (Supplementary Fig. S5).

We conclude that 9q32-q33.1 genes deregulated in the resistant tumors can either be up- or downregulated, and provide either resistance or sensitivity to cisplatin. Moreover, the mechanisms of response seem to be conserved through evolution rather than be specific of human cells or tumors.

DL-threo-PDMP, a competitive inhibitor of GCS, resensitizes refractory TGCT and EOC orthoxenografts to cisplatin

As a proof-of-concept of our approach to search novel therapeutic strategies for overcoming cisplatin resistance, we decided to dig into the therapeutic value of one of these genes/proteins at the preclinical level. *GCS* was chosen on the grounds that: (i) displays increased mRNA expression in all cisplatin refractory orthoxenografts and (ii) there are specific inhibitors for GCS available, some of which are currently in clinical use for other pathologies (32, 33). First, NSE testicular germ cell line SuSaS and its paired cisplatin-resistant SuSaR were used as cellular models to corroborate the functional relationship among GCS expression/activity and cisplatin resistance in TGCTs. Significant differences among protein levels of GCS were observed between both cell lines, being more abundant in resistant cells (Fig. 4A, top). Transfected SuSaS cells overexpressing GCS (Fig. 4A, bottom) displayed a significant cisplatin-resistant increase (5-fold; Fig. 4B), while shRNAi knockdown of the endogenous GSC gene (70% of inhibition) in SuSaR cells correlates with a partial (57.6%) cisplatin resensitization (Fig. 4B). Likewise, the treatment of SuSaR cells with the specific GCS inhibitor DL-threo-PDMP (PDMP) mimics this cisplatin sensitization (44.8%; Fig. 4C). Combined cisplatin + PDMP treatment produces a significant increase in the intracellular levels of ceramide (Fig. 4D). Thus, we demonstrated that impaired GCS expression/activity *in vitro* resensitizes a cisplatin-resistant NSE cell line newly to cisplatin treatment.

Interestingly, cisplatin-refractory engrafted tumors exhibited an increase in GCS activity (Fig. 4D). Then, we treated TGT1XR and TGT38XR daily for 21 days with PDMP. As a single-agent, PDMP did not produce a significant response with respect to the vehicle-treated animals, and no significant

Downloaded from clincancerres.aacrjournals.org on April 16, 2021. © 2018 American Association for Cancer Research.

Published OnlineFirst April 4, 2018; DOI: 10.1158/1078-0432.CCR-17-1898

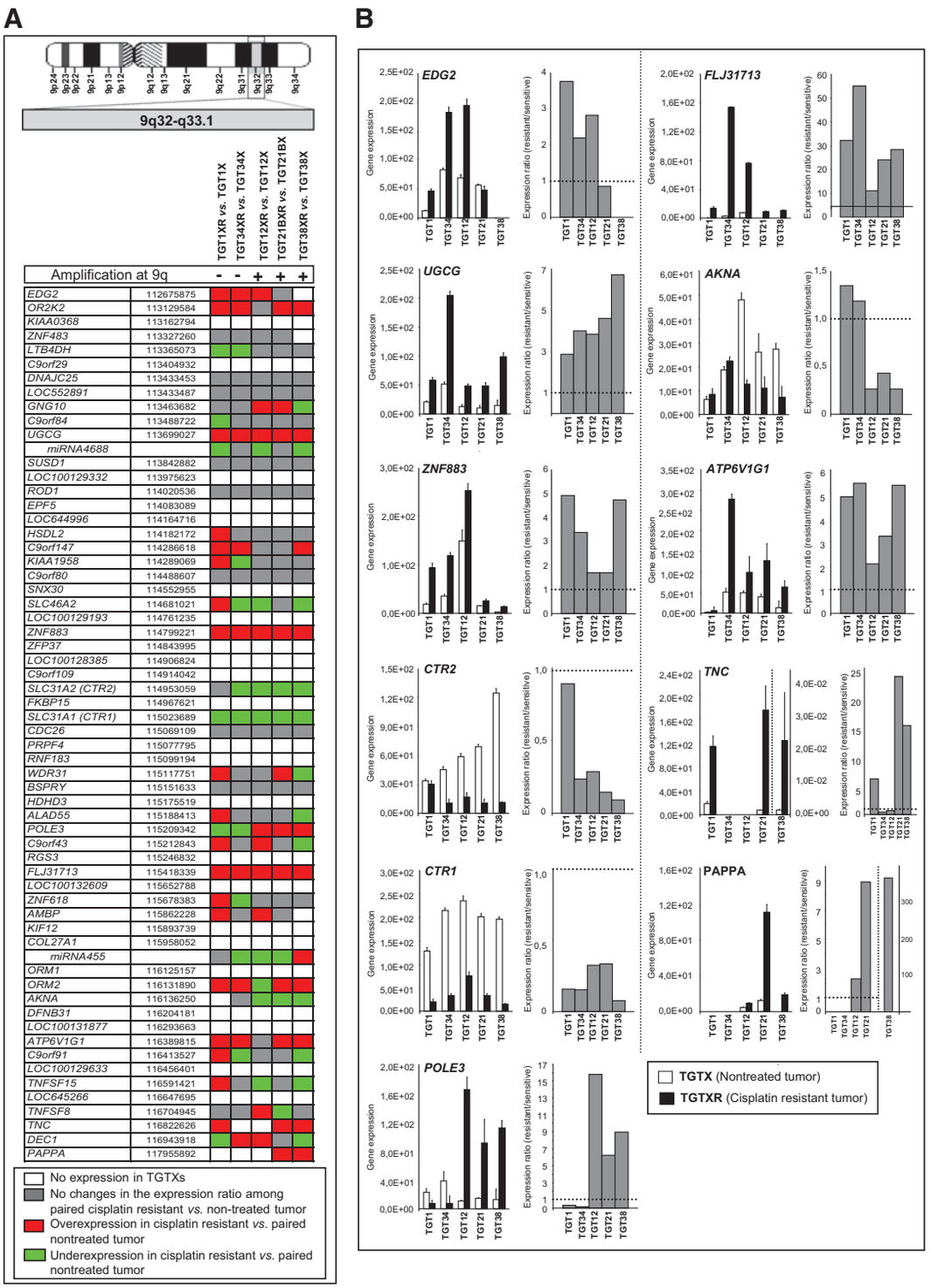

Figure 3.

Differential profiling expression patterns of the 60 genes and two miRNAs annotated on 9q32-q33.1 region determined by qPCR. **A,** Results are presented as changes in the expression levels in cisplatin-refractory tumors relative to the untreated tumors, grouped by 9q32-q33.1 gain status. No expression changes (in gray), underexpression in resistant tumors (in green), overexpression in resistant tumors (in red), and lack of expression in engrafted tumors (in white). **B,** Graphs showing qPCR experiments for relevant genes. For each gene, normalized gene expression (left graph), and the expression ratio among refractory versus sensitive tumors (right graph) are shown. Reactions were performed in triplicate and all data were normalized with endogenous control gene (β-actin).

Downloaded from clincancerres.aacrjournals.org on April 16, 2021. © 2018 American Association for Cancer Research.

Published OnlineFirst April 4, 2018; DOI: 10.1158/1078-0432.CCR-17-1898

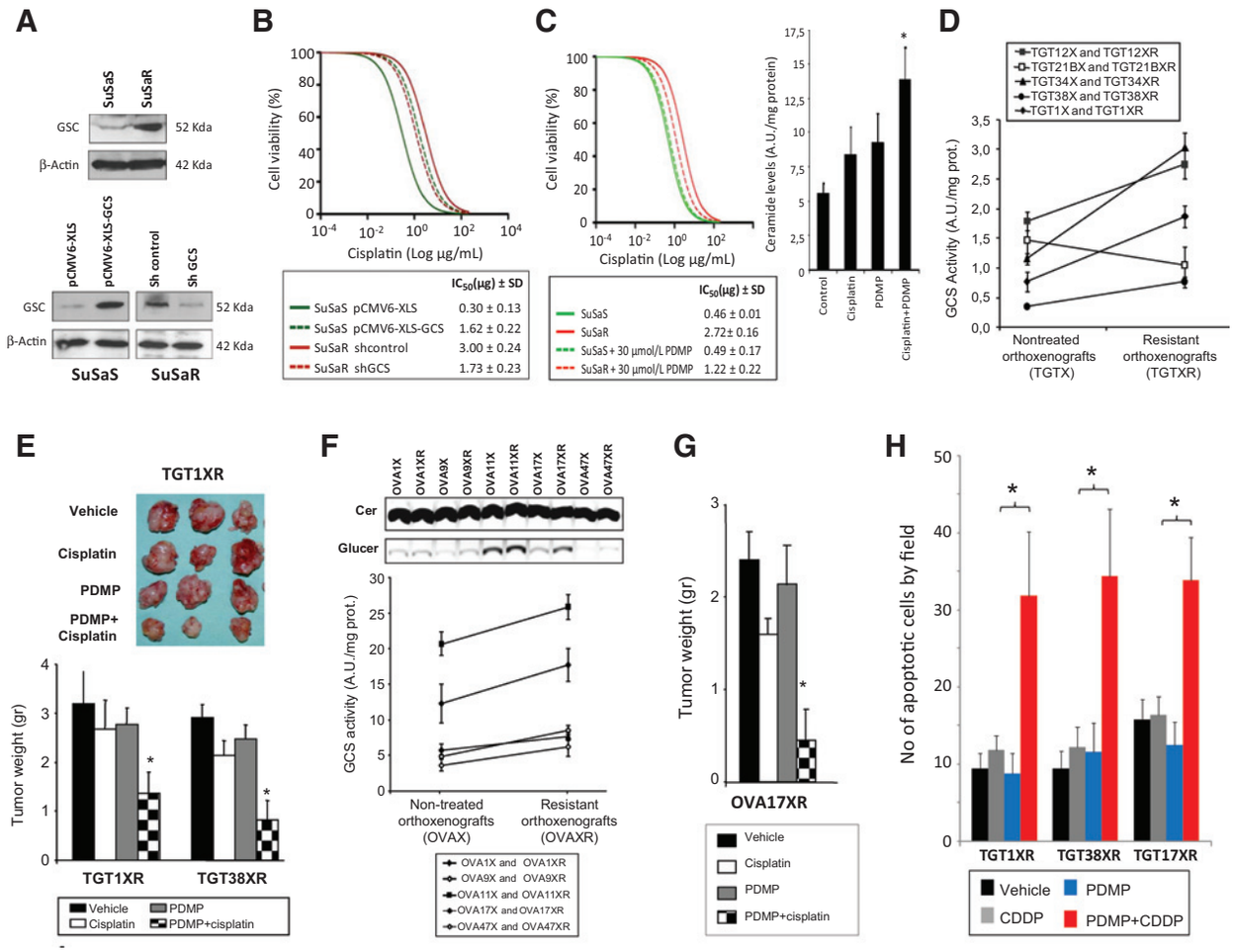

Figure 4.

GCS activity and cisplatin resensitization by DL-threo-PDMP (PDMP) in cisplatin-resistant cell lines and orthoxenografts. **A,** Differential protein expression levels of GCS in SuSaS and paired SuSaR determined by Western blot analysis (left) and GCS transient overexpression in SuSaS cells after transfection with pCMV6-GCS and shRNAi knockdown in SuSaR cells with a mix of four predesigned shRNAs for the human GCS (right). **B,** Cisplatin response of SuSaS cells overexpressing GCS and SuSaR cells with GCS silenced. Each curve represents the average of values from at least three independent experiments and cell proliferation was measured by MTT assay. **C,** Dose–response curves for SuSaS and SuSaR treated with cisplatin and with 30 µmol/L of PDMP [IC_{50} (µmol/L):SuSaS (29.93 ± 0.006)] and SuSaR (28.73 ± 0.054; left). Generation of ceramide was determined in SuSaR cells after treatment with cisplatin, PDMP and for combined cisplatin + PDMP (right). **D,** Activity of GCS in five paired sensitive versus refractory engrafted TGCTs. **E,** Responses of cisplatin-refractory engrafted TGT1XR and TGT38XR tumors to treatment with the GCS inhibitor DL-threo-PMDP. **F,** GCS activity was also determined in six paired sensitive versus refractory orthoxenografts of EOC. Increased levels of glucosylceramide were detected in 5 of 6 resistant cases. **G,** Response of cisplatin-refractory engrafted OVA17XR orthoxenograft (serous tumor) treated with the GCS inhibitor DL-threo-PDMP. **H,** Apoptosis was evaluated by immunostaining of caspase 3 in paraffin sections of residual tumor masses on day 21 of single cisplatin, PDMP, and combined cisplatin + treatments of TGT1XR, TGT38XR, and OVA17XR tumors (22). TGTX, untreated TGCT; TGTXR, cisplatin-refractory TGCT; OVAX, epithelial ovarian tumor; OVAXR, cisplatin-refractory epithelial ovarian tumor (*, $P < 0.05$).

differences were observed among individual PDMP and cisplatin treatments (Fig. 4E). Nevertheless, both tumors experienced significant tumor weight reductions (TGT38XR, 73.5% and TGT1XR, 42.8%) for combined PDMP + cisplatin treatment (Fig. 4E).

Finally, we asked whether the identified association among GCS and cisplatin resistance happens in other tumors commonly treated with cisplatin. Thus, GCS expression/activity was also determined in a panel of five paired cases of sensitive and cisplatin-resistant orthoxenografts of epithelial ovarian cancer (EOC) generated in our lab following the same described approach (22). In 4 of 5 (83.3%) serous tumors, a median increase of 52.5% ± 9.4% GCS activity was observed in the resistant orthoxenografts with respect to its paired sensitive tumors (Fig. 4F). Furthermore, PDMP treatment of OVA17XR, having high levels of GCS activity, has a cisplatin resensitizing effect (Fig. 4G; tumor weight reduction of 76.5% in combined cisplatin + PDMP treatment).

Together, the GCS inhibitor PDMP resensitizes cisplatin-refractory orthoxenografts to cisplatin treatment, providing a promising therapeutic opportunity for treatment of refractory cases; being a strong preclinical rationale for further clinical trials.

Downloaded from clincancerres.aacrjournals.org on April 16, 2021. © 2018 American Association for Cancer Research.

Published OnlineFirst April 4, 2018; DOI: 10.1158/1078-0432.CCR-17-1898

PDMP-induced tumor response is mediated by proapoptotic features in germ cell tumors and ovarian cancer

Next, we investigated whether tumor response mechanisms induced by PDMP associated with proapoptotic induction features. Thus, apoptotic drug induction was assessed in TGT1XR, TGT38XR, and OVA17XR by immunodetection in paraffin-embedded tissues of caspase-3, an early and specific apoptotic marker. In the three orthoxenografts, no significant differences for the proapoptotic induced effect were observed for the single treatments with respect to vehicle group (Fig. 4H). Whereas, for combined PDMP + cisplatin treatment, significant increase in the apoptosis levels was observed in the three tumors respect to cisplatin group (TGT1XR 2.7-fold, $P = 0.0016$; TGT38XR 2.81-fold, $P = 0.0011$; and for OVA17XR 2.06-fold, $P = 0.0002$).

Discussion

Establishment of advanced preclinical models of phenocopying patients' primary tumor features in terms of phenotype, genotype, and response to chemotherapy is a basic step on the way to identifying novel therapeutic targets and for testing antitumoral treatments. Here, we report the generation of an important collection of NSE TGCTs engrafted orthotopically in nude mice, keeping features of primary tumors including sensitivity to cisplatin. In our study, we have used five of those original tumors and their corresponding orthoxenografts that developed cisplatin resistance *in vivo*. Our methodology to induce cisplatin-resistant tumors includes exposure to an increasing concentration of cisplatin through five cycles. Such cisplatin treatment does not occur in the clinic, but in our hands was previously very efficient to generate cisplatin-resistant orthotopic tumors derived from EOC (22). Engrafting patient tumor tissues orthotopically into immunodeficient mice (termed "orthoxenografts or PDOX") are state-of-the-art preclinical models that may contribute to reduce the high rate of failure in translating preclinical results to patients. Among the orthoxenografts used in this study, we previously reported TGT1X, TGT38X, and also its paired resistant TGT38XR as tools to support the preclinical value of sunitinib and lapatinib in TGCT treatments (20, 21, 34). Likewise, other orthoxenografts of EOC and lung cancer have been used to evaluate potential patients' treatments (22, 35, 36).

In 1998, Rao and colleagues provided the first evidence of chromosomal amplification associated with cisplatin resistance by comparing unpaired GCTs obtained from relapse-free patients with chemotherapy-resistant tumors (37). Differently, our study compared resistant and sensitive tumors with the same genetic background and we identified fewer recurrent genomic changes across the different refractory tumors. Still, both studies found amplifications in similar regions at chromosomes 9 and 15. Other studies have identified distinct chromosomal imbalances upon cisplatin exposure suggesting that gains and losses of chromosomal regions are genome instability events whose specific influence in cisplatin resistance acquisition needs to be unraveled. Our study suggests that these genomic imbalances do not have a common impact on gene activities but are hotspots to find genes involved in the response to cisplatin. Thus, *GCS* and *CTR*-1/-2 genes are both deregulated in distinct manner (upregulated and downregulated, respectively) in all five resistant tumors independently of the 9q32-q33.1, indicating that these genes are major drivers of resistance to cisplatin and therefore genomic imbalance of their loci would favor tumor grow in presence of cisplatin. However, we still found a modest clinical correlation between the presence of 9q32-q33.1 gains in tumors and a poor risk defined by shorter OS. Here, we demonstrate that the presence of the 9q32-q33.1 amplification is associated with increased risk of progression and death in one of the largest cohort of patients with metastatic GCTs, of whom 32% are truly refractory to cisplatin treatment. Thus, determining the presence of this amplification can be especially helpful in the good/intermediate prognostic groups and may allow clinicians to include them under more aggressive protocols, or to offer alternative drug treatments. Although it is a single retrospective analysis, it is important to highlight its relevance given the difficulty to obtain representative TGCT series that include patients with a poor prognosis, and refractory tumors.

Regarding specific alterations in gene expression, few genes have been associated with cisplatin resistance in TGCT. Thus, low incidence of mutations in *KRAS*, *AKT1*, *PIK3CA*, and *HRAS* were exclusively identified in resistant GCTs cases, while *FGFR3* mutations occurred with equal frequency in both sensitive and resistant cases (14). Controversy exists about the presence of the b-raf (V600E) mutation in some refractory NSE (14, 38). The whole exome sequence of 42 TGCTs (including SE an NSE, but only some were refractory tumors) pointed few recurrent genetic changes identifying mutations in the XRCC2, which is a gene strongly implicated in defining cisplatin resistance (39). Recently, also by exome sequencing, TP53 pathway alterations including MDM2 amplifications have been described exclusively in patients with cisplatin-resistant tumors and they were particularly prevalent among primary mediastinal NSEs (17). Here we point to six genes within the 9q32-q33.1 region, two of them being (*POLE3* and *AKNA*) specifically deregulated in resistant tumors carrying the 9q32-q33.1 gain. POLE3 is a subunit of the DNA polymerase epsilon that binds DNA in a sequence-independent manner and is part of the CHRAC chromatic-remodeling complex (40). *AKNA* encodes an AT-hook transcription factor (41). The role of these two DNA-binding proteins in response to cisplatin should be studied in the future, but its distinct deregulation in cisplatin-refractory tumors (*POLE3* is upregulated, whereas *AKNA* is downregulated) indicate that their mechanisms of action in response to cisplatin exposure may be different. One explanation for the distinct types of deregulation of genes in 9q32-q33.1 is the frequent amplification of one parental chromosome (of part of it) with loss of the other parental chromosome that led to loss-of-heterozygosity (LOH) in GCTs, but not in other tumor types (42).

Other four genes displayed a deregulated expression in cisplatin-resistant orthoxenografts but such deregulation was not associated with the presence of the 9q32-q33.1 gain. One of them is CTR1, which encodes a copper transporter that has previously been associated to cellular mechanisms of resistance to cisplatin (33, 34). ZNF883 encodes a zinc finger protein that may be involved in transcriptional regulation and FLJ31713 is an uncharacterized protein. Finally, we experimentally confirmed the fourth gene, the *GCS*, as a target to resensitize tumors refractory to cisplatin.

Targeting GCS, due to its central role in the glycosphingolipid synthesis pathway, has emerged as a novel approach for treating metabolic diseases such as Gaucher, Niemann–Pick, and diabetes. In this context, several GCS inhibitors are in

Downloaded from clincancerres.aacrjournals.org on April 16, 2021. © 2018 American Association for Cancer Research.

Published OnlineFirst April 4, 2018; DOI: 10.1158/1078-0432.CCR-17-1898

clinical use or under development, including miglustat, PDMP, and EXEL-0346 among others (43–45). Recently, it has been reported that GCS inhibition improved sorafenib effectiveness *in vitro* and *in vivo* in experimental hepatocellular carcinoma, recovering drug sensitivity of sorafenib-resistant tumors in mice (46). Thus, the therapeutic value of GCS inhibitors as tool to resensitize cell to drugs may not be only restricted to cisplatin.

We have demonstrated the relevance of GCS activity as a biologic mechanism that mediates tumor cell protection against cisplatin exposure, and they denoted the significance of sphingolipid metabolism through cisplatin-induced tumor cell death. Thus, we hypothesize that PDMP or other GCS inhibitors, blocking the conversion of ceramide to glucosylceramide, should open an important therapeutic window in patients with refractory tumors by exploring the influence of ceramide pools in cisplatin-induced cell-death. Our preclinical results in advanced refractory cisplatin orthoxenografts of both GCTs and EOCs tumor models demonstrate that PDMP resensitizes to cisplatin treatment, providing a firm preclinical rationale of drug repositioning and for developing further clinical trials in the field. Interestingly, the association among GCS activity and cisplatin resistance has recently been reported also for head and neck cancer (47), pointing to a broader usage of GCS inhibitors to treat tumors refractory to cisplatin. Given the rather unspecific mechanisms of action of cisplatin, we believe that strategies to resensitize cisplatin-resistant TGCT orthoxenografts may help to improve the treatment of other tumors types that are unsuccessfully treated with cisplatin (8).

In summary, we report the generation of cisplatin-refractory orthoxenografts of germ cell tumors as preclinical models and demonstrate that this preclinical platform have a great potential to better design future trials for the treatment of patients with cisplatin-resistant/refractory tumors.

Disclosure of Potential Conflicts of Interest

A. Vidal has ownership interests (including patents) at Xenopat S.L. L. Padulles is an employee of Almirall SA. A. Villanueva has ownership interests (including patents) at Xenopat S.L. No potential conflicts of interest were disclosed by the other authors.

Authors' Contributions

Conception and design: J.M. Piulats, A. Vidal, M. Nadal, J.R. Germà, X. García-del-Muro, J. Cerón, A. Villanueva

Development of methodology: J.M. Piulats, A. Vidal, F.J. García-Rodríguez, M. Nadal, À. Aytés, S. Puertas, W. Castillo, P. Muñoz, M. Esteller, G. Capella, L. Farré, J. Cerón, A. Villanueva

Acquisition of data (provided animals, acquired and managed patients, provided facilities, etc.): J.M. Piulats, A. Vidal, C. Muñoz, M. Martínez-Iniesta, L. Padullés, M. Juliachs, V. Moreno, M. Stefanovic, E. Condom, M. Esteller, J.R. Germà, G. Capella, L. Farré, A. Morales, X. García-del-Muro, A. Villanueva

Analysis and interpretation of data (e.g., statistical analysis, biostatistics, computational analysis): J.M. Piulats, A. Vidal, F.J. García-Rodríguez, C. Muñoz, M. Nadal, C. Moutinho, A. Figueras, V. Moreno, M.A. Pujana, J.R. Germà, L. Farré, A. Morales, A. Villanueva

Writing, review, and/or revision of the manuscript: J.M. Piulats, A. Vidal, F.J. García-Rodríguez, C. Moutinho, D.G. Molleví, V. Moreno, J.R. Germà, L. Farré, F. Viñals, X. García-del-Muro, J. Cerón, A. Villanueva

Administrative, technical, or material support (i.e., reporting or organizing data, constructing databases): J.M. Piulats, A. Vidal, M. Martínez-Iniesta, L. Farré

Study supervision: J.M. Piulats, A. Vidal, J.R. Germà, X. García-del-Muro, J. Cerón, A. Villanueva

Acknowledgments

Several authors are grateful recipients of predoctoral fellowships: J.M. Piulats from the AECC and F.J. García-Rodríguez from the Instituto de Salud Carlos III (ISCIII). This study was supported by grants from the Spanish Ministry of Economy and Competitiveness (SAF2002-02265 and FIS: BFU2007-67123; PI10-0222, PI13-01339, and PI16/01898, to A. Villanueva; PI15-00895, to J. Cerón; SAF2013-46063R, to F. Viñals; PI030264, to X. García-del-Muro), Fundació La Marató TV3 (051430, to F. Viñals and X. García-del-Muro), Generalitat de Catalunya (2014SGR364, to A. Villanueva and F. Viñals; FIS09/0059, to A. Morales), cofunded by FEDER funds/European Regional Development Fund (ERDF) — a way to Build Europe. A. Villanueva received a BAE11/00073 grant. We thank the staff of the Animal Core Facility of IDIBELL for mouse care and maintenance.

The costs of publication of this article were defrayed in part by the payment of page charges. This article must therefore be hereby marked *advertisement* in accordance with 18 U.S.C. Section 1734 solely to indicate this fact.

Received July 5, 2017; revised November 22, 2017; accepted March 23, 2018; published first April 4, 2018.

References

1. Bray F, Ferlay J, Devesa SS, McGlynn KA, Møller H. Interpreting the international trends in testicular seminoma and nonseminoma incidence. Nat Clin Pract Urol 2006;3:532–43.
2. Ferlay J, Soerjomataram I, Dikshit R, Eser S, Mathers C, Rebelo M, et al. Cancer incidence and mortality worldwide: sources, methods and major patterns in GLOBOCAN 2012. Int J Cancer 2015;136:E359–86.
3. Ruf CG, Isbarn H, Wagner W, Fisch M, Matthies C, Dieckmann K-P. Changes in epidemiologic features of testicular germ cell cancer: age at diagnosis and relative frequency of seminoma are constantly and significantly increasing. Urol Oncol 2014;32:33.e1–6.
4. Beyer J, Albers P, Altena R, Aparicio J, Bokemeyer C, Busch J, et al. Maintaining success, reducing treatment burden, focusing on survivorship: highlights from the third European consensus conference on diagnosis and treatment of germ-cell cancer. Ann Oncol 2013;24:878–88.
5. Funt SA, Feldman DR, Bosl GJ. The management of advanced germ cell tumors in 2016: the Memorial Sloan Kettering approach. Oncology 2016;30:653–64.
6. Lorch A, Neubauer A, Hackenthal M, Dieing A, Hartmann JT, Rick O, et al. High-dose chemotherapy (HDCT) as second-salvage treatment in patients with multiple relapsed or refractory germ-cell tumors. Ann Oncol 2010;21:820–5.
7. Kollmannsberger C, Nichols C, Bokemeyer C. Recent advances in management of patients with platinum-refractory testicular germ cell tumors. Cancer 2006;106:1217–26.
8. Varmus H, Harlow E. Science funding: provocative questions in cancer research. Nature 2012;481:436–7.
9. Koychev D, Oechsle K, Bokemeyer C, Honecker F. Treatment of patients with relapsed and/or cisplatin-refractory metastatic germ cell tumours: an update. Int J Androl 2011;34:e266–73.
10. Houldsworth J, Korkola JE, Bosl GJ, Chaganti RS. Biology and genetics of adult male germ cell tumors. J Clin Oncol 2006;24:5512–8.
11. Galluzzi L, Vitale I, Michels J, Brenner C, Szabadkai G, Harel-Bellan A, et al. Systems biology of cisplatin resistance: past, present and future. Cell Death Dis 2014;5:e1257.
12. Shen D-W, Pouliot LM, Hall MD, Gottesman MM. Cisplatin resistance: a cellular self-defense mechanism resulting from multiple epigenetic and genetic changes. Pharmacol Rev 2012;64:706–21.
13. Honecker F, Wermann H, Mayer F, Gillis AJ, Stoop H, Van Gurp RJ, et al. Microsatellite instability, mismatch repair deficiency, and BRAF

Downloaded from clincancerres.aacrjournals.org on April 16, 2021. © 2018 American Association for Cancer Research.

Published OnlineFirst April 4, 2018; DOI: 10.1158/1078-0432.CCR-17-1898

mutation in treatment-resistant germ cell tumors. J Clin Oncol 2009;27: 2129–36.
14. Feldman DR, Iyer G, Van Alstine L, Patil S, Al-Ahmadie H, Reuter VE, et al. Presence of somatic mutations within PIK3CA, AKT, RAS, and FGFR3 but not BRAF in cisplatin-resistant germ cell tumors. Clin Cancer Res 2014; 20:3712–20.
15. Juliachs M, Muñoz C, Moutinho CA, Vidal A, Condom E, Esteller M, et al. The PDGFRβ-AKT pathway contributes to CDDP-acquired resistance in testicular germ cell tumors. Clin Cancer Res 2014;20:658–67.
16. Koster R, van Vugt MA, Timmer-Bosscha H, Gietema JA, de Jong S. Unravelling mechanisms of cisplatin sensitivity and resistance in testicular cancer. Expert Rev Mol Med 2013;15:e12.
17. Bagrodia A, Lee BH, Lee W, Cha EK, Sfakianos JP, Iyer G, et al. Genetic determinants of cisplatin resistance in patients with advanced germ cell tumors. J Clin Oncol 2016;34:4000–7.
18. Hidalgo M, Amant F, Biankin AV, Budinská E, Byrne AT, Caldas C, et al. Patient-derived xenograft models: an emerging platform for translational cancer research. Cancer Discov 2014;4:998–1013.
19. Byrne AT, Alférez DG, Amant F, Annibali D, Arribas J, Biankin AV, et al. Interrogating open issues in cancer precision medicine with patient-derived xenografts. Nat Rev Cancer 2017;17:254–68.
20. Juliachs M, Castillo-Ávila W, Vidal A, Piulats JM, Garcia Del Muro X, Condom E, et al. ErbBs inhibition by lapatinib blocks tumor growth in an orthotopic model of human testicular germ cell tumor. Int J Cancer 2013; 133:235–46.
21. Castillo-Avila W, Piulats JM, Garcia Del Muro X, Vidal A, Condom E, Casanovas O, et al. Sunitinib inhibits tumor growth and synergizes with cisplatin in orthotopic models of cisplatin-sensitive and cisplatin-resistant human testicular germ cell tumors. Clin Cancer Res 2009;15: 3384–95.
22. Vidal A, Muñoz C, Guillen M, Moreto J, Puertas S, Martinez-Iniesta M, et al. Lurbinectedin (PM01183), a New DNA minor groove binder, inhibits growth of orthotopic primary graft of cisplatin- resistant epithelial ovarian cancer. Clin Cancer Res 2012;18:5399–411.
23. Selzer RR, Richmond TA, Pofahl NJ, Green RD, Eis PS, Nair P, et al. Analysis of chromosome breakpoints in neuroblastoma at sub-kilobase resolution using fine-tiling oligonucleotide array CGH. Genes Chromosomes Cancer 2005;44:305–19.
24. Grande L, Bretones G, Rosa-Garrido M, Garrido-Martin EM, Hernandez T, Fraile S, et al. Transcription factors Sp1 and p73 control the expression of the proapoptotic protein NOXA in the response of testicular embryonal carcinoma cells to cisplatin. J Biol Chem 2012;287:26495–505.
25. Hogan B, Fellous M, Avner P, Jacob F. Isolation of a human teratoma cell line which expresses F9 antigen. Nature 1977;270:515–8.
26. Morales A, París R, Villanueva A, Llacuna L, García-Ruiz C, Fernández-Checa JC. Pharmacological inhibition or small interfering RNA targeting acid ceramidase sensitizes hepatoma cells to chemotherapy and reduces tumor growth *in vivo*. Oncogene 2007;26:905–16.
27. Fléchon A, Culine S, Théodore C, Droz J-P. Pattern of relapse after first line treatment of advanced stage germ-cell tumors. Eur Urol 2005;48:957–64.
28. Albers P, Albrecht W, Algaba F, Bokemeyer C, Cohn-Cedermark G, Horwich A, et al. Guidelines on testicular cancer. Eur Urol 2005;48: 885–94.
29. Lemaire MA, Schwartz A, Rahmouni AR, Leng M. Interstrand cross-links are preferentially formed at the d(GC) sites in the reaction between cis-diamminedichloroplatinum (II) and DNA. Proc Natl Acad Sci U S A 1991;88:1982–5.
30. Szklarczyk D, Morris JH, Cook H, Kuhn M, Wyder S, Simonovic M, et al. The STRING database in 2017: quality-controlled protein–protein association networks, made broadly accessible. Nucleic Acids Res 2017;45:D362–9.
31. Hemmingsson O, Kao G, Still M, Naredi P. ASNA-1 activity modulates sensitivity to cisplatin. Cancer Res 2010;70:10321–8.
32. Patterson MC, Vecchio D, Prady H, Abel L, Wraith JE. Miglustat for treatment of Niemann-Pick C disease: a randomised controlled study. Lancet Neurol 2007;6:765–72.
33. Bennett LL, Mohan D. Gaucher disease and its treatment options. Ann Pharmacother 2013;47:1182–93.
34. Juliachs M, Vidal A, Garcia Del Muro X, Piulats JM, Condom E, Casanovas O, et al. Effectivity of pazopanib treatment in orthotopic models of human testicular germ cell tumors. BMC Cancer 2013;13:382.
35. Alsina-Sanchis E, Figueras A, Lahiguera Á, Vidal A, Casanovas O, Graupera M, et al. The TGFβ pathway stimulates ovarian cancer cell proliferation by increasing IGF1R levels. Int J Cancer 2016;139:1894–903.
36. Ambrogio C, Gómez-López G, Falcone M, Vidal A, Nadal E, Crosetto N, et al. Combined inhibition of DDR1 and Notch signaling is a therapeutic strategy for KRAS-driven lung adenocarcinoma. Nat Med 2016;22:270–7.
37. Rao PH, Houldsworth J, Palanisamy N, Murty VV, Reuter VE, Motzer RJ, et al. Chromosomal amplification is associated with cisplatin resistance of human male germ cell tumors. Cancer Res 1998;58:4260–3.
38. Honecker F, Wermann H, Mayer F, Gillis AJ, Stoop H, van Gurp RJ, et al. Microsatellite instability, mismatch repair deficiency, and BRAF mutation in treatment-resistant germ cell tumors. J Clin Oncol 2009;27:2129–36.
39. Litchfield K, Levy M, Huddart RA, Shipley J, Turnbull C. The genomic landscape of testicular germ cell tumours: from susceptibility to treatment. Nat Rev Urol 2016;13:409–19.
40. Kukimoto I, Elderkin S, Grimaldi M, Oelgeschlä T, Varga-Weisz PD. The histone-fold protein complex CHRAC-15/17 enhances nucleosome sliding and assembly mediated by ACF. Mol Cell 2004;13:265–77.
41. Siddiqa A, Sims-Mourtada JC, Guzman-Rojas L, Rangel R, Guret C, Madrid-Marina V, et al. Regulation of CD40 and CD40 ligand by the AT-hook transcription factor AKNA. Nature 2001;410:383–7.
42. Taylor-Weiner A, Zack T, O 'donnell E, Guerriero JL, Bernard B, Reddy A, et al. Genomic evolution and chemoresistance in germ-cell tumours. Nature 2016;540:114–8.
43. Richards S, Larson CJ, Koltun ES, Hanel A, Chan V, Nachtigall J, et al. Discovery and characterization of an inhibitor of glucosylceramide synthase. J Med Chem 2012;55:4322–35.
44. Huang W-C, Tsai C-C, Chen C-L, Chen T-Y, Chen Y-P, Lin Y-S, et al. Glucosylceramide synthase inhibitor PDMP sensitizes chronic myeloid leukemia T315I mutant to Bcr-Abl inhibitor and cooperatively induces glycogen synthase kinase-3-regulated apoptosis. FASEB J 2011;25: 3661–73.
45. Yu T, Li J, Qiu Y, Sun H. 1-Phenyl-2-decanoylamino-3-morpholino-1-propanol (PDMP) facilitates curcumin-induced melanoma cell apoptosis by enhancing ceramide accumulation, JNK activation, and inhibiting PI3K/AKT activation. Mol Cell Biochem 2012;361:47–54.
46. Stefanovic M, Tutusaus A, Martinez-Nieto GA, Bárcena C, de Gregorio E, Moutinho C, et al. Targeting glucosylceramide synthase upregulation reverts sorafenib resistance in experimental hepatocellular carcinoma. Oncotarget 2016;7:8253–67.
47. Roh J-L, Kim EH, Park JY, Kim JW. Inhibition of glucosylceramide synthase sensitizes head and neck cancer to cisplatin. Mol Cancer Ther 2015;14: 1907–15.

Downloaded from clincancerres.aacrjournals.org on April 16, 2021. © 2018 American Association for Cancer Research.

Published OnlineFirst April 4, 2018; DOI: 10.1158/1078-0432.CCR-17-1898

AACR American Association for Cancer Research

Clinical Cancer Research

Orthoxenografts of Testicular Germ Cell Tumors Demonstrate Genomic Changes Associated with Cisplatin Resistance and Identify PDMP as a Resensitizing Agent

Josep M. Piulats, August Vidal, Francisco J. García-Rodríguez, et al.

Clin Cancer Res 2018;24:3755-3766. Published OnlineFirst April 4, 2018.

Updated version	Access the most recent version of this article at: doi:10.1158/1078-0432.CCR-17-1898
Supplementary Material	Access the most recent supplemental material at: http://clincancerres.aacrjournals.org/content/suppl/2018/04/04/1078-0432.CCR-17-1898.DC1

Cited articles	This article cites 47 articles, 14 of which you can access for free at: http://clincancerres.aacrjournals.org/content/24/15/3755.full#ref-list-1

E-mail alerts	Sign up to receive free email-alerts related to this article or journal.
Reprints and Subscriptions	To order reprints of this article or to subscribe to the journal, contact the AACR Publications Department at pubs@aacr.org.
Permissions	To request permission to re-use all or part of this article, use this link http://clincancerres.aacrjournals.org/content/24/15/3755. Click on "Request Permissions" which will take you to the Copyright Clearance Center's (CCC) Rightslink site.

Downloaded from clincancerres.aacrjournals.org on April 16, 2021. © 2018 American Association for Cancer Research.